

Synthesis and characterization of $\text{Ce}_{0.8}\text{Sm}_{0.2}\text{O}_{1.9}$ nanopowders using an acrylamide polymerization process

ZHENG Yingping (郑颖平)¹, WANG Shaorong (王绍荣)², WANG Zhenrong (王振荣)², WU Liwei (邬理伟)¹, SUN Yueming (孙岳明)¹

(1. School of Chemistry and Chemical Engineering, Southeast University, Nanjing 211189, China; 2. Shanghai Institute of Ceramics, Chinese Academy of Sciences, Shanghai 200050, China)

Received 11 May 2009; revised 10 July 2009

Abstract: $\text{Ce}_{0.8}\text{Sm}_{0.2}\text{O}_{1.9}$ (SDC) nanopowders were synthesized by an acrylamide polymerization process. The XRD results showed that SDC powders prepared at 700 °C possessed a cubic fluorite structure. Transmission electron microscopy (TEM) indicated that the particle sizes of powders were in the range of 10–15 nm. A 98.3% of theoretical density was obtained when the SDC pellets were sintered at 1350 °C for 5 h, indicating that the powders had good sinterability. The conductivity of the sintered SDC ceramics was 0.019 S/cm at 600 °C and the activation energy was only 0.697 eV. Furthermore, a unit cell was fabricated from the powders and the maximum power density of 0.169 W/cm² was achieved at 700 °C with humidified hydrogen as the fuel and air as the oxidant.

Keywords: acrylamide polymerization; doped ceria; solid oxide fuel cell; sintering; electrical conductivity; rare earths

Cerium oxide-based materials have attracted increasing interest as the electrolyte for solid oxide fuel cells (SOFCs), especially for intermediate temperature SOFCs (ITSOFCs, 600–800 °C), due to their high ionic conductivity^[1–8]. For example, $\text{Ce}_{0.8}\text{Sm}_{0.2}\text{O}_{1.9}$ shows high ionic conductivity of around 0.1 S/cm, which is three times higher than that of the conventional 8YSZ (8 mol.% yttria stabilized zirconia, 3×10^{-2} S/cm) at 800 °C^[3,5,9].

In general, nano-sized powders possess high sintering ability, and the particle size of powders greatly depends on the synthesis route. Many methods are available for the preparation of ultrafine homogeneous doped ceria powders, for instance, glycine-nitrate process^[10,11], citrate-nitrate gel synthesis^[12,13], carbonate coprecipitation method^[14], oxalate coprecipitation route^[11,15,16], homogeneous precipitation process^[17], and hydrothermal process^[18].

In this study, we investigated the synthesis and properties of $\text{Ce}_{0.8}\text{Sm}_{0.2}\text{O}_{1.9}$ (SDC) nanocrystalline powders via an acrylamide sol-gel process. In this process, a stable precursor solution of strongly chelated cations was obtained by controlling the amount of ligand and the pH at first. Then the solution was easily gelled by in situ formation of polyacrylamide gel. Fine and nano-sized powders were obtained by directly decomposing this hydrous gel through thermal treatment. Furthermore, the property of a unit cell fabricated from as-prepared powders was also studied.

1 Experimental

1.1 Preparation

The starting materials were commercial CeO_2 powder and Sm_2O_3 powder (purity: 99.9%; Sinopharm Chemical Reagent Co., Ltd., China). They were weighed according to a molar ratio of 8:2, dissolved in dilute nitrate acid separately, and then mixed with 10 equivalents of EDTA. A clear solution was made by slowly adding dilute ammonia under stirring, and pH of the solution was around 8. Then the monomers, acrylamide and N, N'-methyleneacrylamide (6 g and 1 g per 100 ml of solution, respectively) were added to the above solution, and then the mixture was heated at 80–90 °C to produce the polyacrylamide gel.

The gel was dried at 120 °C overnight in an oven, and calcined at 700 °C for 4 h after being pulverized in an agate mortar to prepare crystalline SDC powders. The SDC powders were pressed into pellets and sintered in air on an alumina board at 1350 °C for 5 h. The sintered pellets were approximately 25 mm in diameter and 0.35 mm in thickness.

1.2 Characterization

The crystal structure of the powders was investigated with X-ray diffraction (Shimadzu XD-3A) using Cu K α radiation. The data were recorded at a scanning rate of 5 (°)/min with a scanning step size of 0.02°. The morphology of the SDC powder was studied with a transmission electron microscope (TEM, JEM-2000EX). The sintering shrinkage was measured with a dilatometer (NETZSCH DIL 402C) from room temperature to 1500 °C. The microstructure analysis of the

sintered pellets was carried out using a scanning electron microscope (SEM, Hitachi X-650). The relative density of the sintered pellets was determined by standard Archimedes' method.

The ionic conductivity was measured using two-probe impedance spectroscopy. Platinum paste was applied to both sides of the sintered pellets and heated at 800 °C for 2 h. Measurements were performed in air using an electrochemical workstation (IM6eX, Zahner) in the temperature range 600–900 °C. The values of conductivity at different temperatures were calculated with Eq. (1):

$$\sigma = \frac{L}{RS} \quad (1)$$

where L is the thickness of a pellet, S the area of a pellet (S=1/4 D², D is the diameter), and R the resistance of a pellet at different temperatures.

The electrochemical characterization of a planar single cell was performed with humidified hydrogen as the fuel and air as the oxidant at 600–700 °C using the electrochemical workstation. The anode slurry consisting of 50 wt.% NiO-50 wt.% SDC and cathode slurry consisting of 50 wt.% La_{0.8}Sr_{0.2}MnO₃(LSM)-50 wt.% SDC were deposited by a screen-printing technique onto the separate sides of SDC pellet, which was air-dried and then fired at 1000 °C for 2 h in air. Platinum mesh was placed on top of the anode and the cathode to act as current collectors.

2 Results and discussion

2.1 Powder characteristics

Fig. 1 shows XRD pattern of calcined SDC powder at 700 °C for 4 h with an acrylamide polymerization route. The powder has a fluorite structure, and its pattern is indexed on a cubic cell, space group F23 with lattice parameters of a=b=c=0.5430 nm, α=β=γ=90°.

TEM image of the SDC nanoparticles is shown in Fig. 2. It can be seen that the nanoparticle is well-crystallized with average grain size of 12 nm; and the particles are slightly agglomerated, which may be due to the partial sintering while the exothermic reactions occur.

Fig. 3 shows the sintering curve of the compact powder sample. It can be seen that the linear shrinkage begins to de-

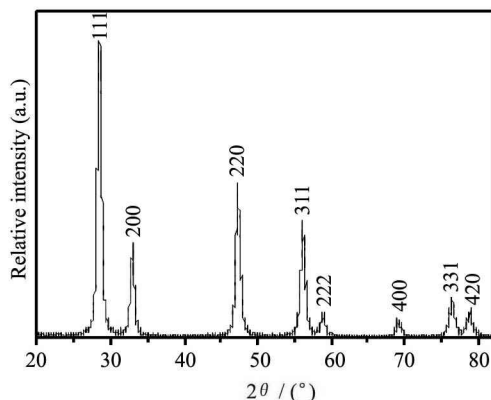


Fig. 1 XRD pattern of SDC powder

scend after 700 °C. A maximum shrinkage of the sample occurs at near 1400 °C. With further increasing of the temperature, the sintering curve begins to rise. Therefore, the sintering temperature of the SDC was chosen between 1350–1400 °C.

2.2 Characterization of sintered SDC pellets

A typical SEM image of the SDC pellet sintered at 1350 °C for 5 h (Fig. 4(a)) reveals a dense and homogeneous microstructure, and the average grain size is 1–2 μm. Fig. 4(b) presents the microstructure of a fractured section of the pellet. The pellet is basically dense although there are closed pores of submicron-size at the grain boundaries. The relative density of SDC pellet was found to be 98.3% by the standard Archimedes' method.

The ionic conductivity was measured using two-probe impedance spectroscopy. The conductivity data were fitted with the Arrhenius Eq. (2):

$$\sigma = \sigma_0 \exp\left(-\frac{E_a}{kT}\right) \quad (2)$$

where σ_0 , E_a , k and T are the conductivity, pre-exponential factor, activation energy, Boltzmann constant and absolute temperature, respectively. Fig. 5 presents the Arrhenius plots for the sintered SDC pellet prepared by different methods. The ionic conductivity of the pellet prepared by acrylamide polymerization method is 0.019 S/cm at 600 °C, and the activation energy is 0.697 eV. As comparison, the data of pellets prepared by glycine-nitrate method and citrate-nitrate method are also shown in Fig. 5.

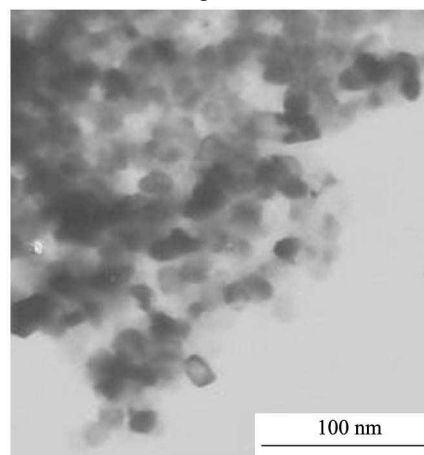


Fig. 2 TEM image of SDC powder

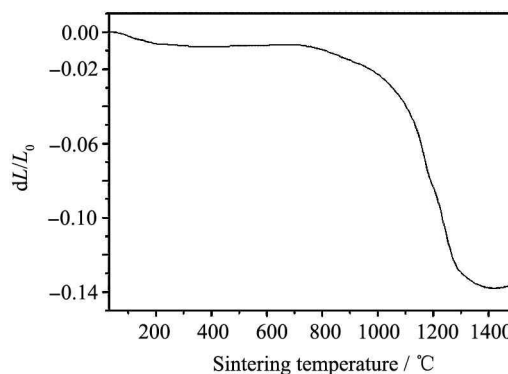


Fig. 3 Sintering curve of the synthesized powder compact sample

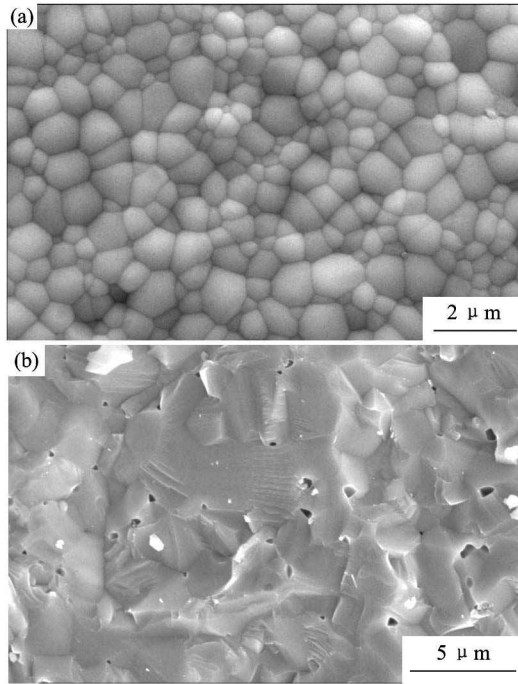


Fig. 4 SEM micrographs of SDC sintered at 1350 °C for 5 h
(a) Surface; (b) Fracture

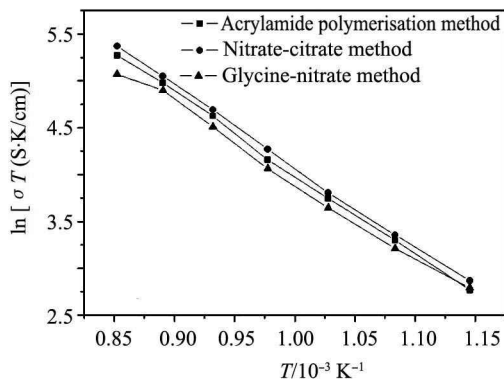


Fig. 5 Arrhenius plots for SDC pellets sintered at 1350 °C for 5 h from powders prepared by different methods

From Fig. 5, it can be found that pellets prepared by acrylamide polymerization method have a lower activation energy and higher conductivity. This result shows that the acrylamide polymerization synthesis is an effective method to prepare doped ceria powders with an excellent electrical performance. Acrylamide gel consists of long polymeric chains, crosslinked to create an organic 3D tangled network where a solution of the respective cations is soaked. Polymerization of the gel proceeds with the way of a chain reaction, the first step of which is the combination of an initiator with the acrylamide, which is thereby activated. As the chain of polyacrylamide grows, the active site shifts to its free end. *N,N'*-methylene diacrylamide, which contains two acrylamide units joined through $-\text{CONH}_2$ group via a methylene group, can link two growing chains. Hence, diacrylamide enables the formation of cross-linked chains, resulting in a complex topology with loops, branches, and interconnections^[19]. Meanwhile the complexation of cations in solution by EDTA permits the mixing of species at a molecular level

and avoids the occurrence of unwanted precipitation. So this method allows preparing uniformly doped ceria powders.

2.3 Cell test results

The cell structure consists of a porous NiO-SDC anode, a dense SDC electrolyte and a porous LSM-SDC composite cathode. The electrochemical performance of as-prepared unit cell was characterized. I-V curves and power densities are shown in Fig. 6(a), and its impedance spectra measured at an open circuit condition for the cell are shown in Fig. 6(b). The measured results are also listed in Table 1.

From Fig. 6(a), it can be found that I-V curves are non-linear, which indicates the presence of a significant polarization at the electrode/electrolyte interface. As the temperature rises, the current density and power density rise. A maximum power density of 0.169 W/cm² is achieved at 700 °C. This value is a little low, but it must be noticed that the thickness of the SDC electrolyte is 350 μm.

From Table 1, it is very clear that the values of electrolyte resistance, R_{e1} , and electrode polarization resistance, $R_{p,a+c}$, have increased significantly along with the increase in the OCV values. Meanwhile, the values of R_{e1} , $R_{p,a+c}$, and OCV decrease with the increase of temperature. The electrolyte resistance (R_{e1}) have decreased from 1.247 to 0.556 Ω·cm² as temperature increases from 600 to 700 °C.

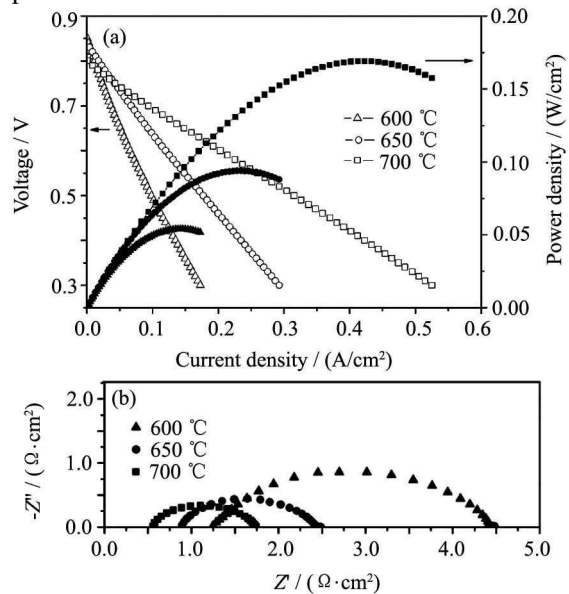


Fig. 6 I-V curves of a single cell at different temperatures (a), and impedance spectra measured at an open circuit condition for the single cell (b)

Table 1 Cell performance and cell resistances*

Temperature/ °C	OCV/ V	MPD/ (W/cm ²)	R_{e1} / (Ω·cm ²)	$R_{p,a+c}$ / (Ω·cm ²)	R_{e1} / (Ω·cm ²)
600	0.856	0.054	1.247	3.210	4.457
650	0.835	0.094	0.891	1.561	2.452
700	0.805	0.169	0.556	1.188	1.744

* OCV: open circuit voltage, MPD: maximum power density, R_{e1} : electrolyte ohmic resistance from EIS, $R_{p,a+c}$: electrode polarization resistance from EIS, R_{e1} : cell resistance from EIS ($R_{e1}=R_{e1}+R_{p,a+c}$)

In comparison with R_{el} of cells with thin SDC electrolytes ($10\ \mu\text{m}$)^[20], the relative high value of R_{el} may be related to the thicker electrolyte pellet. As shown in Table 1, the electrode polarization resistance ($R_{\text{p(a+c)}}$) is dominant in the total resistance of the cell (R_{cell}), which is decreased from 3.210 to 1.188 cm^2 as temperature increases from 600 to 700 °C. Therefore, a better performance of the unit cell can be achieved at 700 °C. In order to further improve the cell performance, it is necessary to decrease the thickness of the electrolyte pellets and enhance catalytic activity of the electrode materials to lower the R_{cell} of unit cells.

3 Conclusions

$\text{Ce}_{0.8}\text{Sm}_{0.2}\text{O}_{1.9}$ powder of 12 nm in average grain size was successfully synthesized by an acrylamide polymerization process. The SDC powder exhibited high sinterability, high conductivity, and low conduction activation energy. With an electrolyte pellet of 350 μm thick, a fuel cell with humidified hydrogen as the fuel and air as the oxidant was assembled and a maximum power density of 0.169 W/cm^2 was obtained at 700 °C. It is believed that SDC powders synthesized by this method would be a promising electrolyte material for intermediate temperature SOFCs.

References:

- [1] Eguchi K. Ceramic materials containing rare earth oxides for solid oxide fuel cell. *Journal of Alloys and Compounds*, 1997, 250: 486.
- [2] Inoue T, Setoguchi T, Eguchi K, Arai H. Study of a solid oxide fuel cell with a ceria-based solid electrolyte. *Solid State Ionics*, 1989, 35: 285.
- [3] Yahiro H, Baba Y, Eguchi K, Arai H. High temperature fuel cell with ceria-yttria solid electrolyte. *Journal of the Electrochemical Society*, 1988, 135: 2077.
- [4] Tompsett G A, Sammes N M, Yamamoto O. Ceria-yttria-stabilized zirconia composite ceramic systems for applications as low-temperature electrolytes. *Journal of the American Ceramic Society*, 1997, 80: 3181.
- [5] Mogensen M, Sammes N M, Tompsett G A. Physical, chemical and electrochemical properties of pure and doped ceria. *Solid State Ionics*, 2000, 129: 63.
- [6] Eguchi K, Setoguchi T, Inoue T, Arai H. Electrical properties of ceria-based oxides and their application to solid oxide fuel cells. *Solid State Ionics*, 1992, 52: 165.
- [7] Hibino T, Hashimoto A, Inoue T, Tokuno J I, Yoshida S I, Sano M. A low-operating-temperature solid oxide fuel cell in hydrocarbon-air mixtures. *Science*, 2000, 288: 2031.
- [8] Sahibzada M, Steele B C H, Zheng K, Rudkin R A, Metcalfe I S. Development of solid oxide fuel cells based on a $\text{Ce}(\text{Gd})\text{O}_{2-x}$ electrolyte film for intermediate temperature operation. *Catalysis Today*, 1997, 38: 459.
- [9] Yahiro H, Baha Y, Eguchi K, Arai H. Oxygen ion conductivity of the ceria-samarium oxide system with Fluorite. *Journal of Applied Electrochemistry*, 1988, 18: 527.
- [10] Peng R R, Xia C R, Fu Q X, Meng G Y, Peng D K. Sintering and electrical properties of $(\text{CeO}_2)_{0.8}(\text{Sm}_2\text{O}_3)_{0.1}$ powders prepared by glycine-nitrate process. *Materials Letters*, 2002, 56: 1043.
- [11] Peng R R, Xia C R, Peng D K, Meng G Y. Effect of powder preparation on $(\text{CeO}_2)_{0.8}(\text{Sm}_2\text{O}_3)_{0.1}$ thin film properties by screen-printing. *Materials Letters*, 2004, 58: 604.
- [12] Peng C, Zhang Y, Cheng Z W, Cheng X, Meng J. Nitrate-citrate combustion synthesis and properties of $\text{Ce}_{1-x}\text{Sm}_x\text{O}_{2-x/2}$ solid solutions. *Journal of Materials Science: Materials in Electronics*, 2002, 13: 757.
- [13] Song X W, Peng J, Zhao Y W, Zhao W G, An S L. Synthesis and electrical conductivities of $\text{Sm}_2\text{O}_3\text{-CeO}_2$ systems. *Journal of Rare Earths*, 2005, 23: 167.
- [14] Moria T, Drönnanb J, Wang A Y, Aucheerlonie G, Li J, Yago A. Influence of nano-structural feature on electrolytic properties in Y_2O_3 doped CeO_2 system. *Science and Technology of Advanced Materials*, 2003, 4: 213.
- [15] Gao R F, Mao Z Q. Sintering of $\text{Ce}_{0.8}\text{Sm}_{0.2}\text{O}_{1.9}$. *Journal of Rare Earths*, 2007, 25: 364.
- [16] Van Herle J, Horita T, Kawada T, Sakai N, Yokokana H, Dokiya M. Low temperature fabrication of (Y, Gd, Sm)-doped ceria electrolyte. *Solid State Ionics*, 1996, 86-88: 1255.
- [17] Djuricic B, Pickering S. Nanostructured cerium oxide: preparation and properties of weakly-agglomerated powders. *Journal of the European Ceramic Society*, 1999, 19: 1925.
- [18] Dikmen S, Shuk P, Greenblatt M, Gomez H. Hydrothermal synthesis and properties of $\text{Ce}_{1-x}\text{Gd}_x\text{O}_2$ solid solutions. *Solid State Sciences*, 2002, 4: 585.
- [19] Sin A, Odier P. Gelation by acrylamide, a quasi-universal medium for the synthesis of fine oxide powders for electroceramic applications. *Advanced Materials*, 2000, 12: 649.
- [20] Zhang X, Robertson M, Deces-Petit C, Qu W, Kesler O, Manic R, Ghosh D. Internal shorting and fuel loss of a low temperature solid oxide fuel cell with SDC electrolyte. *Journal of Power Sources*, 2007, 164: 668.